Reactions (^{7}Li, ^{7}Li), (^{7}Li, ^{6}Li), and (^{7}Li, ^{6}He) on the deformed target ^{24}Mg at $E_{^7\text{Li}}$ = 34 MeV*

G. E. Moore, K. W. Kemper, and L. A. Charlton

Department of Physics, The Florida State University, Tallahassee, Florida 32306

(Received 19 November 1974)

Angular distributions for the single nucleon transfer reactions ^{24}Mg(^{7}Li, ^{6}Li)^{25}Mg and ^{24}Mg(^{7}Li, ^{6}He)^{25}Al have been measured to study the effects of target deformation on heavy-ion transfer reactions at $E_{^7\text{Li}}$ = 34 MeV. Elastic and inelastic scattering angular distributions have also been measured for ^{7}Li + ^{24}Mg at the same energy. Optical model fits to the elastic scattering data were good in the diffraction region, but they overestimated the cross section at forward angles. Coupled channels calculations, which coupled the ground and first excited states of ^{24}Mg with ^{7}Li in its ground state, yielded deformation lengths that are in agreement with those obtained from light-ion scattering measurements. The single nucleon transfer data were compared to exact finite range distorted wave Born approximation calculations. While the extracted spectroscopic factors are in reasonable agreement with those obtained from light-ion works, the calculations are out of phase with the data. Parameter variations by as much as 20% did not resolve this problem. The cross sections for transitions to the j-forbidden $\frac{7}{2}^+$ (1.61 MeV) states in ^{25}Al and ^{25}Mg were smaller relative to the allowed transitions than observed in corresponding light-ion single nucleon transfer reactions.

> NUCLEAR REACTIONS ^{24}Mg(^{7}Li, ^{7}Li$_{0,1}$)^{24}Mg$_{0,1}$, E = 34 MeV; measured $\sigma(\theta)$;
> deduced optical model parameters and deformation lengths for ^{24}Mg.
> ^{24}Mg(^{7}Li, ^{6}Li), (^{7}Li, ^{6}He) E = 34 MeV; measured $\sigma(\theta)$; deduced S from finite
> range DWBA analysis.

I. INTRODUCTION

Studies of single nucleon transfer reactions have proven to be a valuable tool for gathering nuclear spectroscopic information. However, considerable uncertainty exists in the magnitude of the extracted spectroscopic factors for highly deformed nuclei since reactions involving these nuclei are often influenced by inelastic excitation in the incident and exit channels. Recent attempts[1-5] to analyze light ion reactions in the $2s$-$1d$ shell with the inclusion of inelastic excitations have resulted in considerable confusion. The fits to the shapes of the experimental angular distributions have been in general improved by including inelastic excitation, while the magnitudes of the calculations have had to be adjusted by as much as a factor of 10, with different renormalizations for each state studied.

The use of heavy-ion reactions greatly increases the number of single nucleon transfer reactions which can be used to extract spectroscopic factors. These extracted spectroscopic factors can provide a check on the light-ion information unless the heavy-ion reactions introduce too many additional complications into the analysis. A recent study of

the ^{62}Ni(^{7}Li, ^{6}He)^{63}Cu reaction[6] indicated that finite range distorted wave Born approximation (FRDWBA) calculations were able to describe the shape of the angular distributions and their magnitude. In the present work, the ^{24}Mg(^{7}Li, ^{6}Li)^{25}Mg and ^{24}Mg-(^{7}Li, ^{6}He)^{25}Al reactions have been measured to study the additional complications which occur when deformed nuclei take part in the reaction. Elastic and inelastic scattering of ^{7}Li by ^{24}Mg has been measured in addition to the transfer data. The elastic scattering data have been analyzed with the optical model, while the inelastic scattering data with ^{7}Li in its ground state and ^{24}Mg in its first excited state were analyzed using the coupled channels method. The data for the ground and first excited states of ^{24}Mg with ^{7}Li in its first excited state were not analyzed but are presented. The single nucleon transfer data were analyzed with the exact FRDWBA. The extracted spectroscopic factors are compared with those obtained from light-ion reaction studies.

II. EXPERIMENTAL PROCEDURE

The Florida State University super FN tandem Van de Graaff accelerator was used to accelerate

a $^7Li^{+3}$ beam obtained from a Heinicke ion source[7] to 34 MeV. The ^{24}Mg targets were made by vacuum evaporation of 99.9% pure ^{24}Mg onto 5 $\mu g/cm^2$ carbon foils. Typical target thicknesses were 150 $\mu g/cm^2$. The data for angles greater than 15° were obtained in a scattering chamber[8] using two Si surface barrier counter telescopes and a monitor counter. Data forward of 15° were taken using a single counter telescope at the image position of a quadrupole spectrometer (QDO).[9] The resolution was typically 80–100 keV for data obtained in the QDO and 120 keV for data obtained in the scattering chamber. A monitor counter was used for normalization of the different runs. Only one particle type at a time was focused, and the band pass of the QDO allowed for a uniform detection efficiency for levels within half an MeV of the focused energy. The azimuthal angle subtended was 1° for angles 10° and greater and 0.55° for angles less than 10° . The data taken in the QDO were normalized at 15° to data taken in the scattering chamber for the purpose of obtaining absolute cross sections. The counter telescopes consisted of 25 and 40 μm ΔE counters and 690 μm E counters. The ΔE and E signals were amplified and then pulse height analyzed by analog to digital converters (ADC) interfaced via CAMAC to an EMR-6130 computer. The stored ΔE-E coincidences were displayed on a storage scope where gates could be drawn around the various particle types with an interactive light pen. After establishing the gates

around the regions of interest, the data were accumulated and sorted into linear spectra on line. The ^7Li, ^6Li, and ^6He spectra were accumulated simultaneously for data taken in the scattering chamber.

The extremely high ^7Li count rate at angles less than 15° resulted in an incomplete separation of ^7Li from ^6Li. This "leak through" resulted in a high background in the ^6Li spectra. It was not possible in general to take ^6Li spectra forward of 5° lab, and the ground state transition to ^{25}Mg in the reaction $^{24}Mg(^7Li, ^6Li)^{25}Mg$, which has a Q value of 0.076 MeV, could not be separated from the elastic scattering forward of 10° lab. Forward angle ^6Li and ^6He spectra are shown in Fig. 1. Data were taken in 2.5° increments from 1° to 40° for the $(^7Li, ^6He)$ reaction and from 5° to 57.5° for the $(^7Li, ^6Li)$ reaction. Spectra for other angles are shown in Fig. 2. An energy calibrated pulser was used to determine an upper limit of 5 $\mu b/sr$ for the $^{24}Mg(^7Li, ^6He)^{25}Al$ reaction at 165° lab.

The elastic scattering of ^7Li by ^{24}Mg was measured at $E_{^7Li} = 34$ MeV in the angular range 7.5° to 65° lab in 2.5° steps. A typical elastic scattering spectrum is shown in Fig. 3 where each ^7Li peak appears as a doublet corresponding to ^7Li in its ground and first excited state. In order to minimize the experimental difficulties which occur for the high elastic count rates obtained at forward angles, the QDO was used to measure the $^7Li^{+2}$ yield between 7.5° and 15°. In order to obtain the
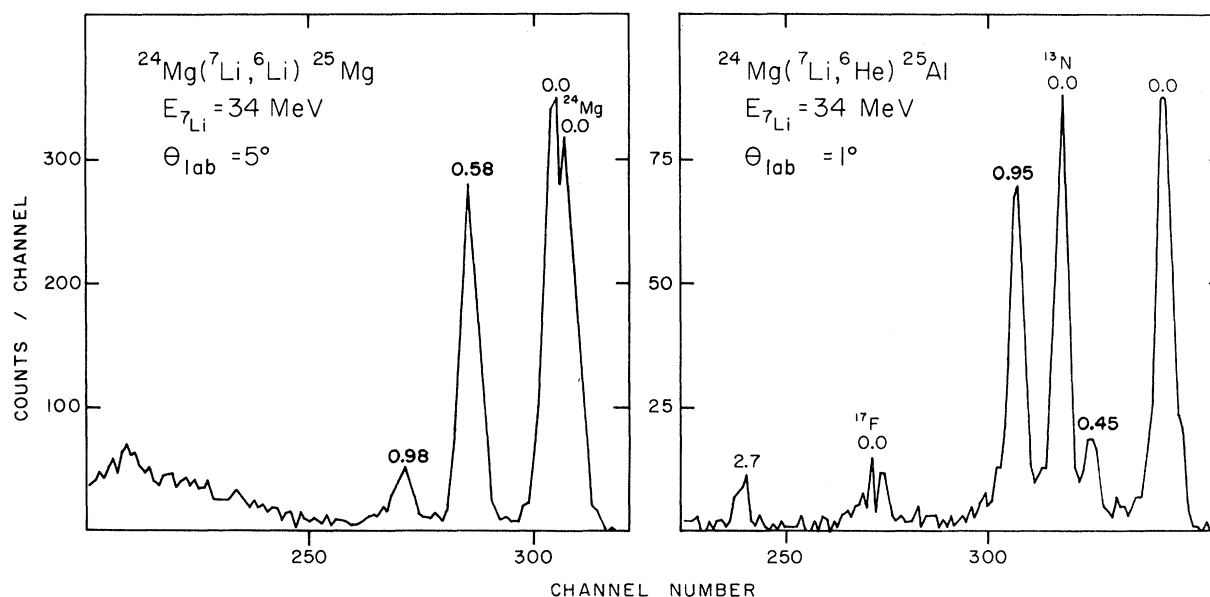

FIG. 1. Forward angle spectra taken in the quadrupole spectrometer. The quadrupole spectrometer focus was set for 0.5 MeV excitation in the residual nucleus. The contribution to the ^6Li spectra from the incomplete separation of the ^7Li elastic events from the ^6Li events at forward angles can be seen.

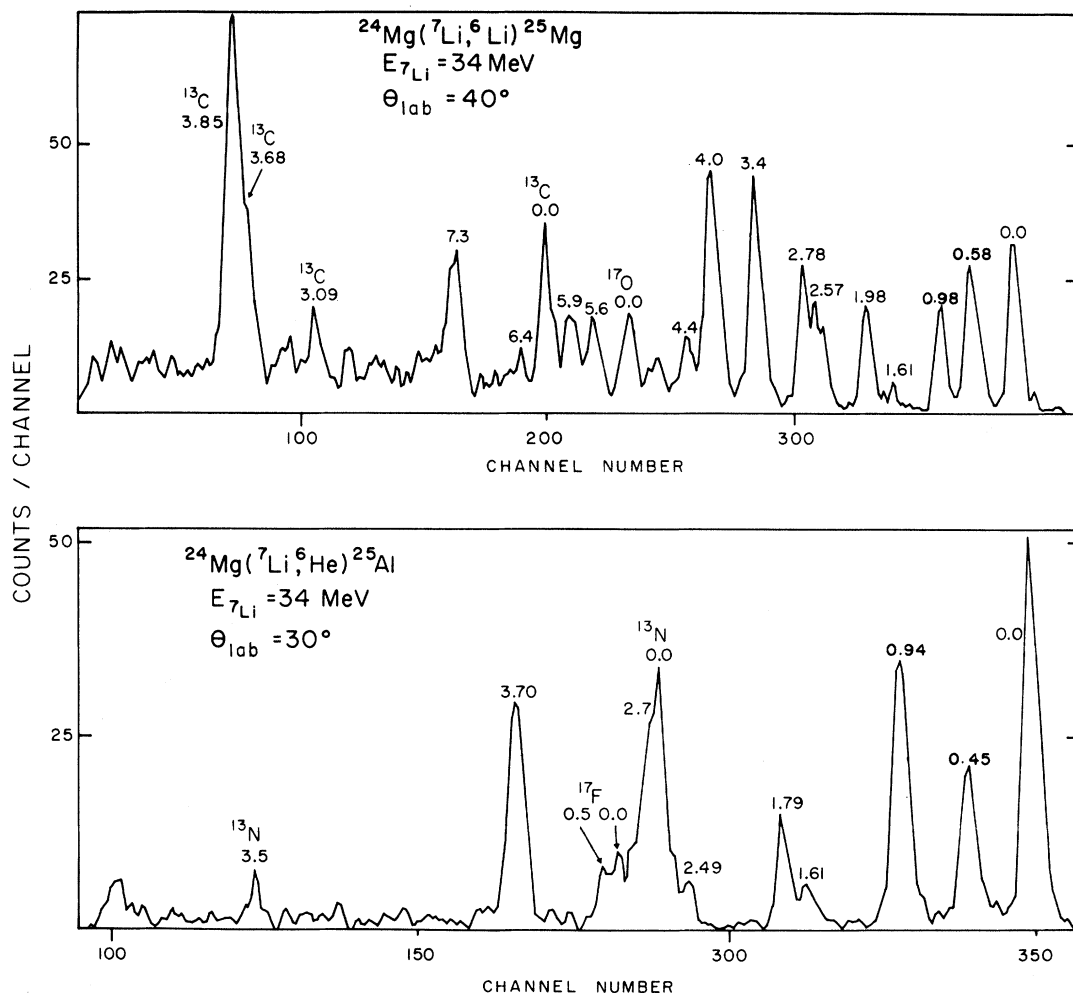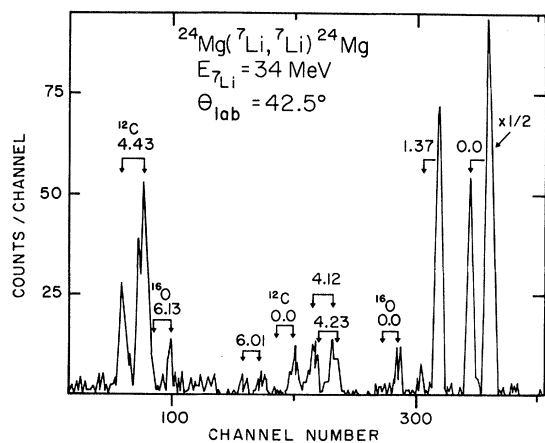FIG. 2. Sample transfer reaction spectra taken in a scattering chamber.

FIG. 3. Sample ^{24}Mg(^{7}Li,^{7}Li)^{24}Mg spectrum. The double arrow indicates the spacing between ^{7}Li in its ground and first excited states.

total elastic cross section, it was assumed that the ratio of charge state 2 to charge state 3 did not change for the small change in ejectile energy which occurs in this angular range. This ratio was checked by comparing with data taken in the scattering chamber at 10°, 12.5°, and 15° lab. The two sets of data agreed to better than 3%.

The relative statistical and peak fitting errors in the cross sections are represented by the error bars on the individual data points for the angular distributions. Where no error bars are visible, the dot size exceeds or equals the relative error associated with that point. To obtain absolute cross sections, a weighed foil of thickness 530 ±16 μg/cm² was used to measure elastic scattering in the scattering chamber. The detector solid angle was determined by measuring the dimensions of the collimator and distance from the target. A combination of errors in the charge integration, target thickness, solid angle determination, and counting errors gives an absolute error of 12%.

TABLE I. Optical model parameters. a and b are starting values for the searches.

Particle	Set	U (MeV)	r_r (fm)	a_r (fm)	W (MeV)	r_i (fm)	a_i (fm)	$\beta_2 R$
^{7}Li	a	177.3	1.21	0.78	9.4	2.1	0.85	$\cdots$
^{7}Li	a	214.6	1.21	0.83	14.4	2.1	0.73	$\cdots$
^{7}Li	I	195.3	1.21	0.78	31.2	1.67	0.89	1.49–1.69
^{7}Li	b	49.7	1.78	0.58	8.52	1.78	1.01	$\cdots$
^{7}Li	II	53.2	1.21	0.57	38.7	1.27	1.26	1.28–1.43
^{6}Li	I	208.6	1.21	0.75	19.8	1.79	0.89	$\cdots$
^{6}Li	II	161.9	1.21	0.80	17.3	1.85	0.89	$\cdots$
^{6}Li	III	37.2	1.75	0.65	29.2	1.50	1.14	$\cdots$

III. ELASTIC AND INELASTIC SCATTERING ANALYSIS

A. Elastic scattering

The elastic scattering data were analyzed in terms of the optical model using a modified version of the computer code JIB.[10] The Woods-Saxon potential used in the calculations was of the form

$$V(r) = -U\left[1 + \exp\left(\frac{r - R_r}{a_r}\right)\right]^{-1}$$
$$-iW\left[1 + \exp\left(\frac{r - R_I}{a_I}\right)\right]^{-1} + V_c$$

with

$$R_{r(I)} = r_{r(I)} A_{\text{target}}^{1/3}$$

and

$$V_c = \frac{Z_1 Z_2 e^2}{2 R_c}\left(3 - \frac{r^2}{R_c^2}\right) \quad r \le R_c = 1.3 A_{\text{target}}^{1/3}$$
$$= \frac{Z_1 Z_2 e^2}{r} \quad r > R_c \ .$$

Two sets of optical parameters for ^{7}Li elastic scattering by ^{28}Si obtained by Schumacher et al.[11] were used as starting values for parameter searches. These optical parameters are labeled a in Table I. A third optical Set b, obtained by White and Kemper[6] for ^{7}Li elastic scattering by ^{62}Ni, was also used as a starting value for an optical parameter search. This set was characterized by a much shallower real potential and was used to see if equivalent sets with large and small, potential depths could be obtained.

The optical parameter searches consisted of varying U, a_r, W, r_I, and a_I. Starting Sets a converged to final Set I as listed in Table I. Final Set II resulted from starting Set b. Both final sets give nearly identical fits to the data and are shown in Fig. 4. The tail of the real potential in Set I minus the Coulomb part is similar to the tail of the imaginary potential in Set II. The tail of the imaginary potential in Set I is similar to the tail of the real potential in Set II minus the Coulomb

part. The value of the two real potentials $(V_R = -3.7$ MeV) is the same at $R = 6.7$ fm. For these potentials, the strong absorption radius[12] is $R = 7.1$ fm and the strong absorption partial wave is 19.5. The imaginary potentials for the two potential sets have the same value $(V_I = -2.5$ MeV) at $R = 7$ fm. The calculations give a good description of the data in the diffraction region, while the fit to the data at forward angles was well above the data. This type of fit was also obtained by Schumacher et al.[11] for ^{7}Li elastic scattering by other light nuclei.

B. Inelastic scattering

The angular distribution for the inelastic scattering to the 2^+ (1.37 MeV) state of ^{24}Mg is shown
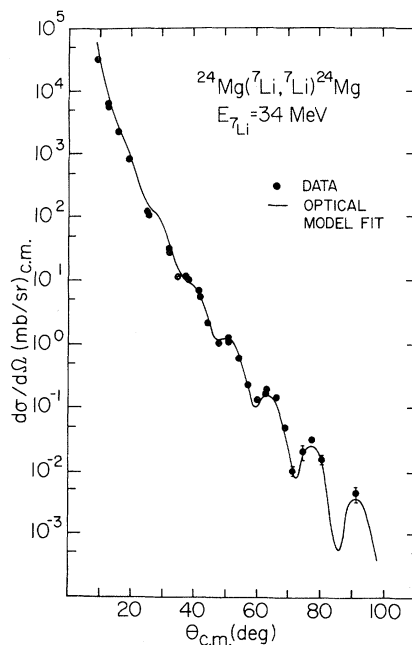

FIG. 4. The elastic scattering angular distribution and optical model fits to the data. The two sets of optical model parameters listed in Table I yielded almost identical fits to the data.

along with the elastic scattering in Fig. 5. As can be seen, the magnitude of the 2^+ cross section is the same order as the ground state for angles greater than 40°. The angular distributions for the scattering to the ground state and first excited state of ^{24}Mg with ^{7}Li in its first excited state are shown in Fig. 6. The magnitude of the cross sections to these states competes in strength with that of the elastic scattering at angles greater than 60°. As seen in Figs. 5 and 6, the first excited state of ^{24}Mg is out of phase with the ground state for both states of ^{7}Li, which is in agreement with the Blair phase rule.[13]

The magnitude of the cross section to the 4^+ (4.12 MeV) member of the ground state rotational band is less than 10 μb/sr over the angular range studied. The 2^+ (4.23 MeV) and 4^+ (6.01 MeV) members of the $K = 2$ γ-vibrational band are even

weaker than the rotational states and could not be extracted.

The large relative magnitude of the inelastic scattering with respect to the elastic scattering makes it necessary to use coupled channels techniques to analyze the inelastic scattering. Only the ground state and first excited state of ^{24}Mg with ^{7}Li in its ground state were coupled in the calculations discussed here. The coupling to the first excited state of ^{7}Li should also be important, but it was not analyzed in the present work. A program which allows coupling to excited states in the residual nucleus and ejectile is presently being developed.[14] The parameters obtained from the optical model analysis were used in the coupled channels calculations performed with the computer code JUPITOR.[15] It was found necessary to use 35 partial waves when coupling the ground state and first excited state. The target nucleus was assumed to be axially symmetric, and the Legendre expansion of the potential was used. Complex form factors were used in the calculation, and the adiabatic approximation was not made. Using β_2 as the only variable, the best simultaneous fits to both states were obtained with β_2 in the range 0.31–0.35 for optical Set I and 0.35–0.39 for optical Set II. The calculations for a β_2 of 0.35 are shown in Fig. 5 along with the data. Variation of
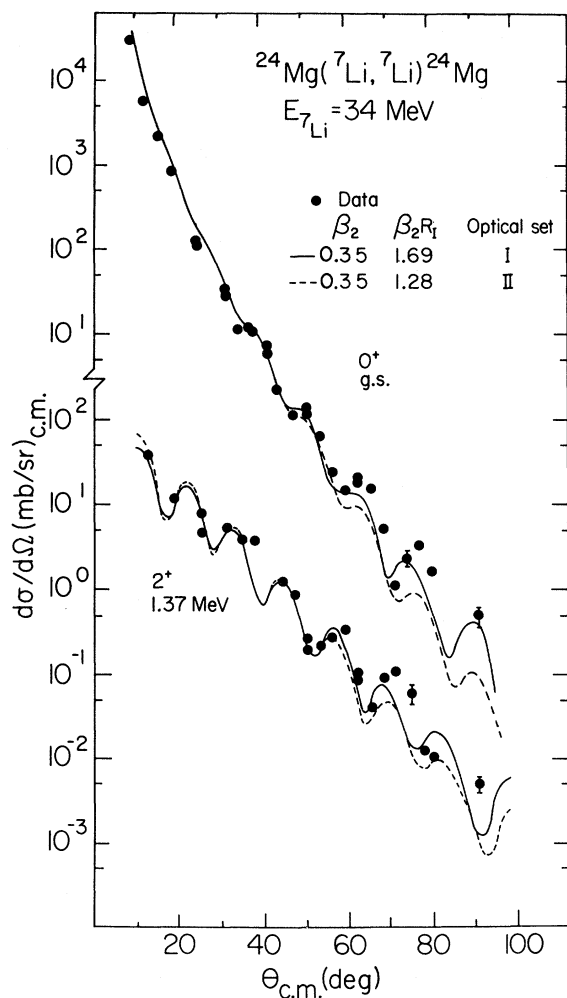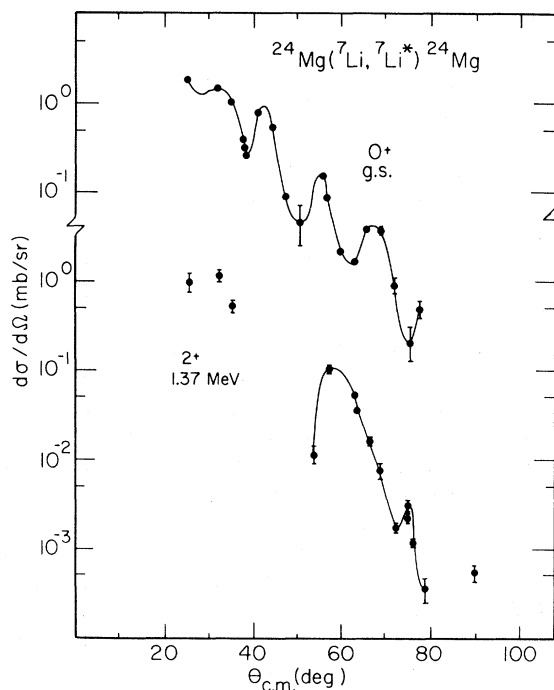

FIG. 5. Angular distributions for ^{24}Mg in its ground and first excited states and ^{7}Li in its ground state. The curves are the results of coupled channels calculations.

FIG. 6. Angular distributions for reactions with ^{7}Li in its first excited state and ^{24}Mg in its ground and first excited states. The curves are to guide the eye.

U and *W* by as much as 20% did not result in appreciably better simultaneous fits to both states. The coupling to the 4^+ (4.12 MeV) state with β_4 $= -0.015$ had little effect on the 0^+ and 2^+ differential cross sections when included in the calculations.

The fits to the 0^+ and 2^+ angular distributions are exceptionally good. A comparison with deuteron elastic and inelastic scattering[3,16] shows that the ^{7}Li elastic and inelastic scattering fits to the shape of the data are as good, if not better, over the angular range studied. In determining the deformation length, $\beta_2 R$, an uncertainty exists as to whether the real or imaginary potential radius should be used for R.[11] It was noted in the previous section that optical potential Set I (II) produced a potential which was dominated by the real (imaginary) potential in the tail region. To determine whether the real or imaginary radius should be used in computing the deformation length, the coupled channels calculations were performed with only a real form factor, and then again with only an imaginary form factor. It was found that the structure and magnitude of the 0^+ and 2^+ angular distributions were determined by the imaginary potential for both optical sets. Consequently, the imaginary radius was used in determining the deformation length, $\beta_2 R_I$. The values so determined were $\beta_2 R_I = 1.49-1.69$ for Set I, and 1.28–1.43 for Set II. These values are in agreement with those obtained from light-ion studies[3,5,16-19] ($\beta_2 R = 1.3-1.9$). Thus, ^{7}Li elastic and inelastic scattering analysis yielded results that were comparable to that obtained from light-ion studies even though

coupling to the first excited state of ^{7}Li was not included.

IV. RESULTS AND ANALYSIS OF THE SINGLE NUCLEON TRANSFER DATA

A typical spectrum for the ^{24}Mg(^{7}Li, ^{6}Li)^{25}Mg reaction is shown in Fig. 2. Angular distributions for all the low-lying states were extracted. The relative strengths of the states populated are similar to those observed in the ^{24}Mg(d,p)^{25}Mg reaction[1-5] except for the comparatively weak population of the $\frac{7}{2}^+$ (1.61 MeV) "*j*-forbidden" state in the ^{7}Li induced reaction. On the basis of the magnitude of the (^{7}Li, ^{6}He) reaction cross section relative to that of the (^{7}Li, ^{6}Li) reaction cross section, the transition to the ^{6}Li, $T = 1$ state should be at least a factor of 10 smaller than the (^{7}Li, ^{6}Li$_{g.s.}$) transition, and, in fact, no peaks could be positively attributed to states of ^{25}Mg with ^{6}Li in the 0^+ (3.56 MeV, $T = 1$) state.

A typical spectrum from the ^{24}Mg(^{7}Li, ^{6}He)^{25}Al reaction is also shown in Fig. 2. A comparison of the spectrum with that from the (^{7}Li, ^{6}Li) reaction illustrates the strong effect that angular momentum mismatch has on the population of states. The s states at 0.45 and 2.50 MeV are much weaker relative to the d states in the (^{7}Li, ^{6}He) reaction, which has a mismatch of $\sim 3.6\hbar$, than in the (^{7}Li, ^{6}Li) reaction, which has a mismatch of $\sim 1.1\hbar$. The cross section to the $\frac{7}{2}^+$ (1.61 MeV), *j*-forbidden state of ^{25}Al is of the order of 20 μb/sr or less. Data for this state were difficult to extract from the spectra because of the low cross section. The cross sections to the $\frac{7}{2}^+$ (1.61 MeV) states of ^{25}Al
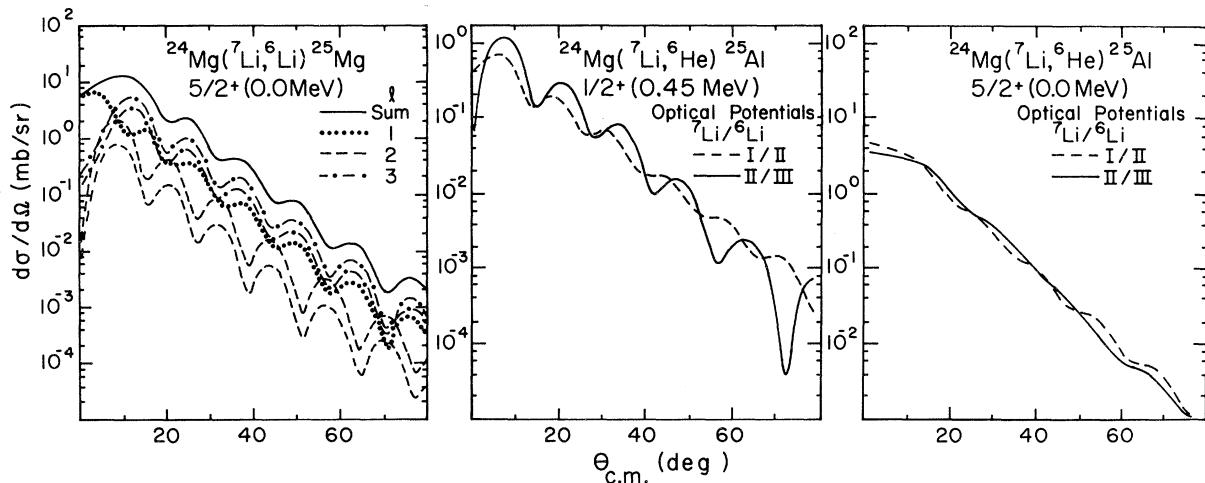

FIG. 7. FRDWBA calculations. The left figure shows the different components of the cross section. For $l = 2$ and 3, contributions from both the $p_{3/2}$ and $p_{1/2}$ configurations of the ^{7}Li $\rightarrow$ ^{6}Li $+n$ system occur. For both l transfers the larger contribution comes from the $p_{3/2}$ component. In the other two figures, calculations with two different combinations of optical parameters are shown.

and ^{25}Mg are about the same size.

The transferred particle in both the ^{24}Mg$(^7Li, ^6Li)$-^{25}Mg and ^{24}Mg$(^7Li, ^6He)^{25}$Al reactions is in a relative p state, which means that finite range DWBA calculations are necessary when analyzing the data with the DWBA. The computer code MERCURY[20] was used to perform the exact finite range DWBA calculations. The selection rules for single nucleon transfer reactions may be written as

$$|L_1 - L_2| \leq l \leq |L_1 + L_2| ,$$

$$|J_1 - J_2| \leq l \leq |J_1 + J_2| ,$$

where

$$\vec{J}_{1(2)} = \vec{L}_{1(2)} + \vec{S}_x .$$

Here, L_1, J_1 (L_2, J_2) are the orbital and total angular momentum of nucleon x with spin S_x when bound to the residual nucleus (projectile) and l is the angular momentum transfer. A set of l transfers is obtained for each configuration of the nucleon x bound to the projectile core. The bound state wave functions were generated with Woods-Saxon potentials. The depths of the potentials were adjusted to give the correct separation energies. The geometrical parameters were fixed at r_0 $= 1.25$ fm, and $a = 0.65$ fm for both bound states and the spin orbit parameter was $\lambda = 25$. The spectroscopic factors were those of Cohen and Kurath.[21]

The two configurations, $p_{3/2}$ and $p_{1/2}$, of ^{6}Li $+n$ allow two angular momentum transfers for the $p_{1/2}$ configuration and three angular momentum transfers for the $p_{3/2}$ configuration, except for $s_{1/2}$ states which have only one l transfer per configuration. All l transfers are added incoherently

to form a total cross section. The effect of having a large number of l transfers is to smooth out the angular distributions. This effect is illustrated in Fig. 7 for the ^{24}Mg$(^7Li, ^6Li)^{25}$Mg reaction to the ground state of ^{25}Mg. For ^{6}He $+p$, a $p_{3/2}$ configuration was assumed.

The optical model parameters used in the calculations are those given in Table I. The ^{6}Li Sets I and II were the best fits to ^{6}Li elastic scattering on ^{26}Mg obtained by Schumacher et al.[11] An optical parameter set for ^{6}Li scattering by ^{63}Cu obtained from White and Kemper[6] was used as a starting point for an optical search using the cross section predicted by ^{6}Li Set I. The optical parameters thus obtained are given as Set III. The ^{7}Li optical parameters are those obtained in this work as discussed earlier.

The calculations for the reaction ^{24}Mg$(^7Li, ^6He)$-^{25}Al to the $\frac{5}{2}^+$ (0.0 MeV) and $\frac{1}{2}^+$ (0.45 MeV) states were used to test the different optical parameter sets since these two states have large spectroscopic factors and are presumably less affected by multistep contributions. The $(^7Li, ^6He)$ reaction was chosen to do test calculations instead of the $(^7Li, ^6Li)$ reaction because the two p configurations present in the $(^7Li, ^6Li)$ reaction greatly increased the computing time. The choice of the $(^7Li, ^6He)$ reaction makes the assumption that the ^{6}He and ^{6}Li optical parameters are similar, which is open to question. However, two previous works[6,11] indicate this substitution is valid.

The angular distribution of the $\frac{1}{2}^+$ state has a great deal of structure due to the single l transfer and should be a severe test of the calculations. Optical Sets I/II and I/I for ^{7}Li/^{6}Li give essentially

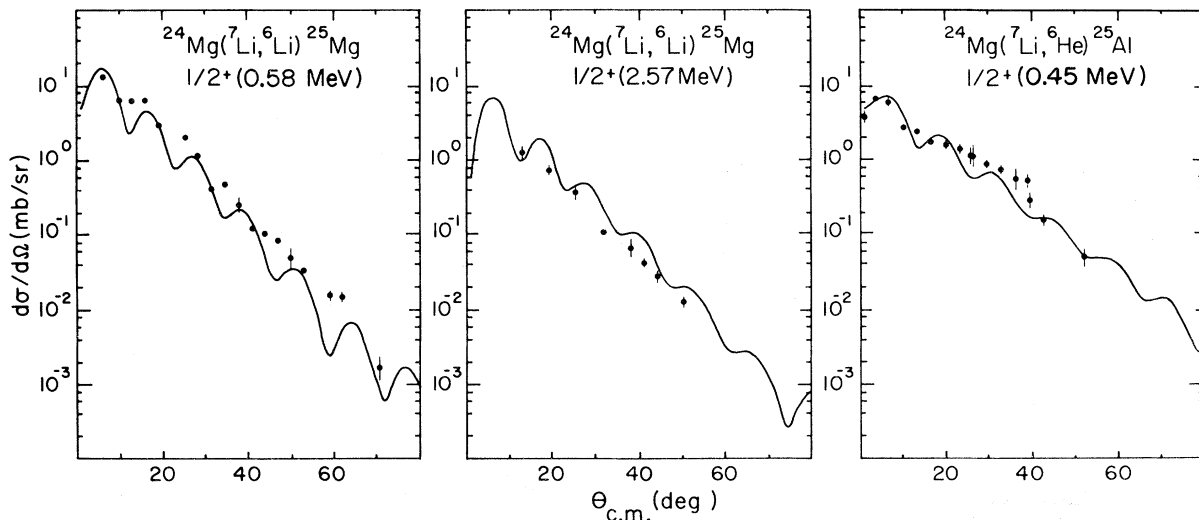FIG. 8. Angular distributions for transitions to $2s_{1/2}$ final states in ^{25}Mg and ^{25}Al. The solid curves are the results of FRDWBA calculations.

identical angular distributions. The angular distributions calculated using optical Sets I/II and II/III are shown in Fig. 7 for the $\frac{5}{2}^+$ and $\frac{1}{2}^+$ states. The slope and magnitude are very similar at forward angles, but the two angular distributions gradually become out of phase. Comparison with the data showed the Sets I/II to give the best fit to the data, and all other calculations to be presented here were performed with optical Sets I/II. Forty-two partial waves were used in the calculations, and it was found necessary after several test calculations to perform the radial integration to 20 fm in 0.1 fm steps. These integration parameters were most important in the case of reactions going to ^{25}Al where the proton is bound to ^{24}Mg by 2.29 MeV or less. Calculations for unbound levels were performed assuming a binding energy of 0.2 MeV.

A. s states

The angular distributions for the $\frac{1}{2}^+$ (0.58 MeV) and $\frac{1}{2}^+$ (2.57 MeV) states of ^{25}Mg are shown in Fig. 8 along with the $\frac{1}{2}^+$ (0.45 MeV) state of ^{25}Al. The data for the $\frac{1}{2}^+$ (0.45 MeV) state of ^{25}Al appear to be fairly structureless except for the first maximum. The finite range DWBA calculation shown in Fig. 8 also does not show a great deal of structure. Even though the angular momentum mismatch of the (^{7}Li, ^{6}He) reaction does not favor the $l=1$ transfer, the FRDWBA calculation gives a reasonable fit to the data.

In the (^{7}Li, ^{6}Li) reaction, the angular momentum mismatch favors the $\frac{1}{2}^+$ states; consequently, the magnitude of the cross section to the two $\frac{1}{2}^+$ states of ^{25}Mg, shown in Fig. 8, is larger than the $\frac{1}{2}^+$ states of ^{25}Al. As stated earlier, the $\frac{1}{2}^+$ (0.58 MeV) state should give an indication as to how well the

FRDWBA calculations are able to fit not only the magnitude of the cross sections but also the details of the shape, since only one l transfer contributes. Although the fits to the data are quite reasonable, they are 4° out of phase. Unfortunately, it was not experimentally possible to extract data at the extreme forward angles to compare with the calculations at the first stripping peak to determine if the calculations were out of phase over the whole angular range. Other combinations of optical parameter sets besides Sets I/II did not yield any better fits to the data. The effect of spin orbit coupling was investigated by including a 10 MeV spin orbit potential in the ^{6}Li channel for the $p_{3/2}$ configuration. The only result was a slight filling in of the minima of the angular distributions. The inability to fit the phase for the $\frac{1}{2}^+$ state in ^{13}C has also recently been reported for the ^{12}C (^{14}N, ^{13}N)^{13}C reaction.[22] As in the ^{12}C + ^{14}N case, the (^{7}Li, ^{6}Li) data give a good fit for $l=0$ transfer, while only $l=1$ is allowed by angular momentum selection rules. There is no explanation for this difficulty at present in either case.

B. d states

The experimental angular distributions for three d states of ^{25}Al are shown in Fig. 9. It is evident that the shape of the angular distributions at forward angles distinguishes between the first $\frac{3}{2}^+$ and $\frac{5}{2}^+$ states of ^{25}Al as noted in a previous paper.[23] The calculations for these states, shown in Fig. 9, reproduce the shape of the angular distributions best at forward angles. The $\frac{5}{2}^+$ state calculation has been plotted with two different normalizations which fit the data from 1°–15° and 15°–35° lab angle. The reaction to the $\frac{5}{2}^+$ (1.80 MeV) state had
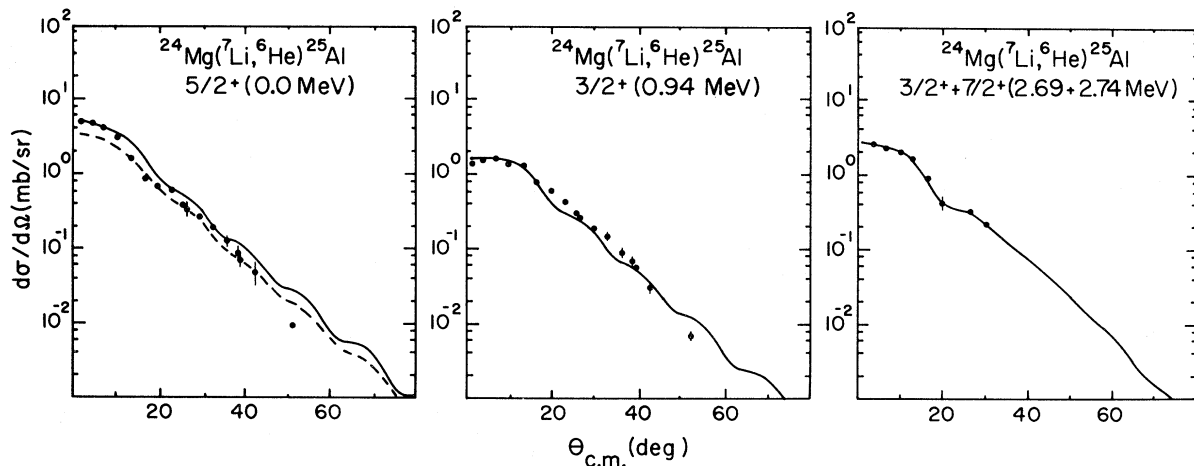

FIG. 9. (^{7}Li, ^{6}He) angular distributions for $1d$ state transitions. The curves are the results of FRDWBA calculations. The solid curves are the result of normalizing the calculations to the data for $\theta < 15°$. The dashed curve is the result of normalizing the calculation to the data for $\theta > 15°$.
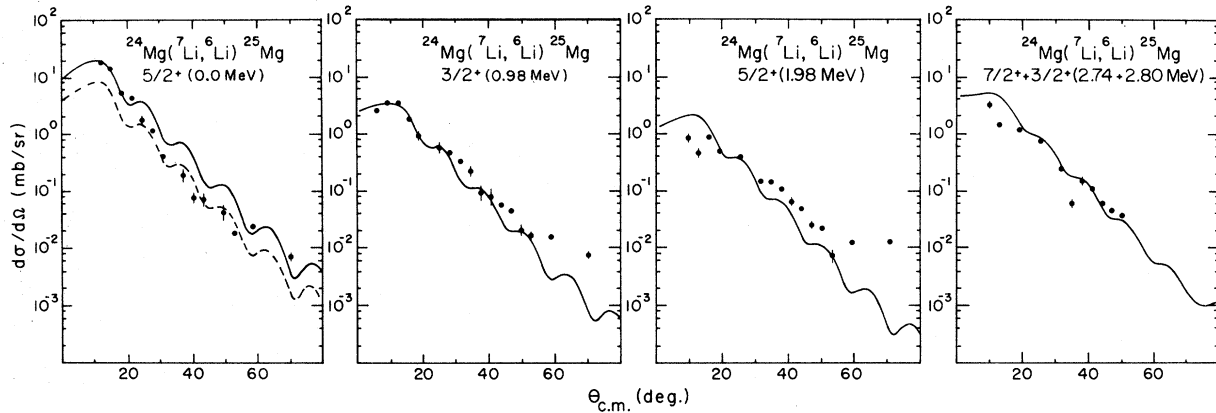
FIG. 10. (^{7}Li,^{6}Li) angular distributions for $1d$ state transitions. The curves are the results of FRDWBA calculations. In the left-most figure, the solid curve has been normalized to the data for $\theta < 15°$ and the dashed curve has been normalized to the data for $\theta > 15°$.

a cross section of 100 μb/sr or less over the angular range where data were taken and could not be reliably extracted. The peak at 2.7 MeV has been assumed to be predominantly the $\frac{3}{2}^+$ (2.69 MeV) state. The fit to the data with this assumption is excellent.

The angular distributions for the first four d states of ^{25}Mg are shown in Fig. 10. It was not possible to take data at forward enough angles to distinguish between the first $\frac{3}{2}^+$ and $\frac{5}{2}^+$ states of ^{25}Mg. The DWBA fits to the $\frac{5}{2}^+$ (0.0 MeV) state are plotted with two normalizations. The shape of all four angular distributions is reproduced reasonably well by the calculations. The weaker $\frac{5}{2}^+$ (1.96 MeV) and $\frac{3}{2}^+$ (2.8 MeV) states vary considerably

from the calculations at forward angles. Forward angle data for the ^{24}Mg$(d,p)^{25}$Mg reaction to the $\frac{5}{2}^+$ (1.96 MeV) state were also found to vary at forward angles.[5,24] This variation may arise from the small spectroscopic strength of this state which would enhance multistep contributions.

C. Negative parity states

The angular distributions for the $\frac{9}{2}^+ + \frac{3}{2}^-$ (3.40 + 3.41 MeV) and $\frac{7}{2}^- + \frac{9}{2}^+$ (3.97 + 4.05 MeV) states of ^{25}Mg and the $\frac{7}{2}^-$ (3.71 MeV) state of ^{25}Al are shown in Fig. 11. The angular distributions for the two states of ^{25}Mg do not have a great deal of structure. It was assumed in the analysis that these
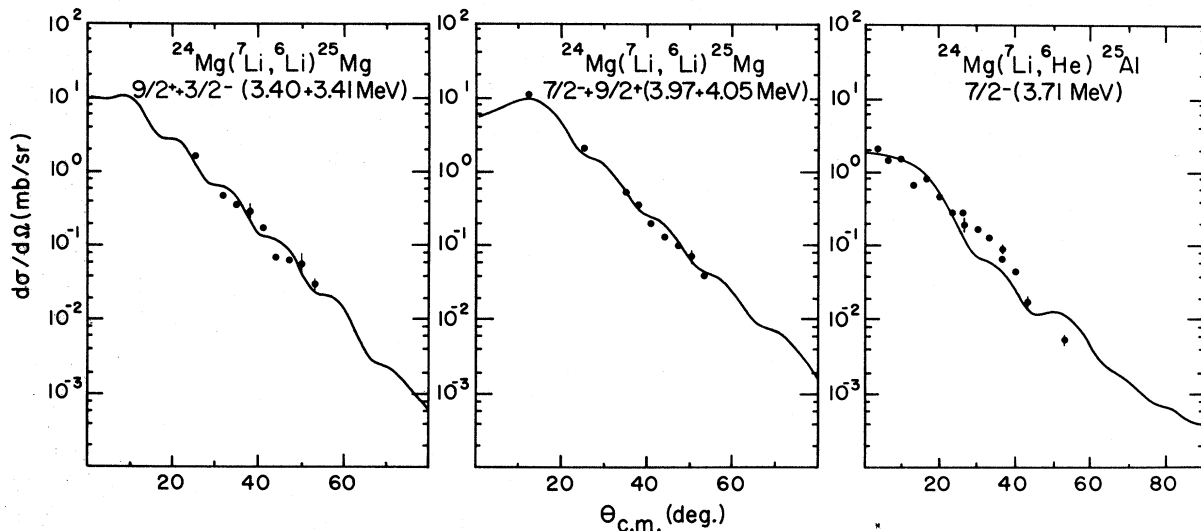

FIG. 11. (^{7}Li,^{6}Li) angular distributions for two groups of states which could not be resolved and the (^{7}Li,^{6}He) transition to the $1f_{7/2}$ unbound level in ^{25}Al at 3.71 MeV. The curves are FRDWBA results. In the (^{7}Li,^{6}Li) calculation, it was assumed the transfer was to a $2p_{3/2}$ and $1f_{7/2}$ final state in the left and center figures, respectively.

states are the $p_{3/2}$ and $f_{7/2}$ single particle states
of ^{25}Mg at 3.41 and 3.97 MeV, respectively. The
calculations for the unbound $\frac{7}{2}^-$ (3.71 MeV) state
of ^{25}Al were very sensitive to the range of the
radial integration and the radial integration was
carried out to 30 fm for the calculation shown in
Fig. 11.

D. g states

The magnitude of the cross sections to the $\frac{7}{2}^+$
states of ^{25}Al and ^{25}Mg at 1.61 MeV are much
smaller than the other states populated in this
reaction. The angular distribution of the ^{25}Mg $\frac{7}{2}^+$
state does not fall off as rapidly as the other
states observed, as seen in Fig. 12. Only three
data points could be extracted for the ^{25}Al $\frac{7}{2}^+$
state, and these are also shown in Fig. 12. For
the FRDWBA calculation, a 130 MeV potential well
depth was needed to bind the proton or neutron in
a $g_{7/2}$ orbit using a 1.25 fm radius for the bound
state of the residual nucleus. The finite range cal-
culations predict that the cross sections to both
$\frac{7}{2}^+$ states are the same order of magnitude with
the same normalization constant. The $\frac{7}{2}^+$ state
cross sections are smaller in magnitude than that
observed in the ^{24}Mg$(d,p)^{25}$Mg reaction, while the
s- and d-state cross sections are about the same
order of magnitude.

E. Spectroscopic factors

The differential cross section as calculated by
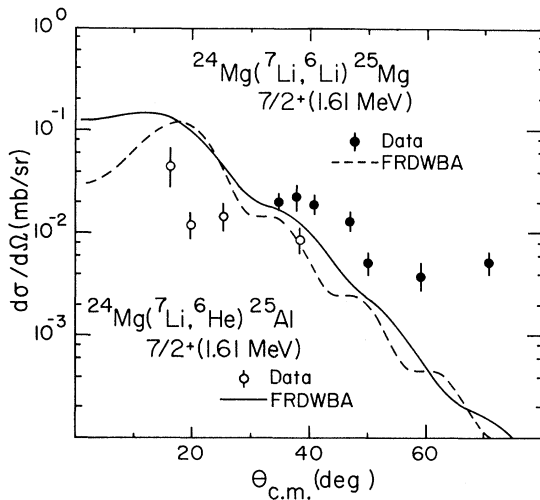the exact finite range DWBA code MERCURY [20]

FIG. 12. Data for the "j-forbidden" $\frac{7}{2}^+$ (1.61 MeV)
transition. The closed circles are (^{7}Li, ^{6}Li) data and
the open circles are (^{7}Li, ^{6}He) data. The curves are
the results of FRDWBA calculations assuming transfer
to a $1g_{7/2}$ final state.

is related to the experimental cross section by

$$\sigma_{exp} = \sum_{i=1}^{N} C_i {}^2S_i \, C_R {}^2S_R \, \sigma_{\text{MERCURY}} \,,$$

where N is the number of configurations of ^{7}Li and
R refers to the single particle configuration of the
residual nucleus. In this work, the absolute spec-
troscopic factor, S_R, was varied to fit the data,
while the ^{7}Li $\rightarrow$ ^{6}Li$+n$ ($S_{p_{3/2}} = 0.431$ and $S_{p_{1/2}}$
$= 0.289$) and ^{7}Li $\rightarrow$ ^{6}He$+p$ ($S_{p_{3/2}} = 0.888$) spectroscop-
ic factors were taken from Cohen and Kurath.[21] A
spectroscopic factor maxima and minima were ob-
tained depending on whether forward angle or back-
ward angle data were to be fitted. The ^{25}Mg ground
state transition, shown in Fig. 10, illustrates the
difficulty in extracting spectroscopic factors for
a rapidly decreasing cross section when the first
stripping peak is not observed, and the calculation
and data are out of phase. The Nilsson coeffi-
cients[24] ($C_{nlj}{}^2$) are related to the absolute spec-
troscopic factors by

$$C_{nlj}{}^2 = \frac{C_R {}^2S_R}{2\langle I_i jK_i \Omega | I_f K_f \rangle {}^2 \langle \phi_f | \phi_i \rangle} \,.$$

The overlap, $\langle \phi_f | \phi_i \rangle$, was taken to be unity. For
both of the single nucleon transfer reactions con-
sidered here

$$C_R {}^2S_R \frac{(2J+1)}{2} = C_{nlj}{}^2 \,,$$

where J is the spin of the residual nucleus. The
Nilsson coefficients obtained from this work are
compared in Table II with Nilsson coefficients
obtained from the ^{24}Mg$(d,p)^{25}$Mg reaction. The
agreement is quite good between the ^{7}Li and deu-
teron induced reactions, except for the ^{25}Mg
ground state, where the data were insufficient to
determine the spectroscopic factor. The Nilsson
coefficients obtained for analog states from the
(^{7}Li, ^{6}Li) and (^{7}Li, ^{6}He) reactions are quite similar.

V. CONCLUSION

The purpose of this work was to investigate the
nature of the ^{7}Li induced single nucleon transfer
reactions on a deformed nucleus. Optical model
parameters were deduced which gave good fits to
the elastic scattering data. A coupled channels
analysis of the elastic and inelastic scattering
data yielded deformation lengths in reasonable
agreement with those obtained from light-ion
studies even though the contribution to the scat-
tering from ^{7}Li in its first excited state was neg-
lected. The optical model parameters were used
in FRDWBA analyses of transitions to states of
^{25}Al and ^{25}Mg. The spectroscopic factors obtained

TABLE II. Experimental Nilsson coefficients for ^{25}Al and ^{25}Mg.

$E_x(^{25}Mg, ^{25}Al)$ (MeV)	J^π	(d,p) [a] $E_d=15$ MeV	(d,p) [b] $E_d=15$ MeV	$(^7Li, ^6Li)$ [c] $E_{^7Li}=34$ MeV	$(^7Li, ^6He)$ [c] $E_{^7Li}=34$ MeV	(d,n) [d] $E_d=7-9$ MeV
0.0 , 0.0	$\frac{5}{2}^+$	0.81	1.10	1.68 (0.76)	0.90 (0.60)	1.74
0.58, 0.45	$\frac{1}{2}^+$	0.39	0.25	0.25 − 0.30 (0.30)	0.34 (0.36)	0.85
0.98, 0.95	$\frac{3}{2}^+$	0.48	0.48	0.34 (0.40)	0.34 (0.40)	0.90
1.61, 1.61	$\frac{7}{2}^+$	...	...	0.01 − 0.08	0.01−0.08	...
1.96, 1.80	$\frac{5}{2}^+$	0.16	0.21	0.07 − 0.14 (0.20)	...	0.60
2.57, 2.50	$\frac{1}{2}^+$	...	0.09	0.20 (0.13)	...	
2.80, 2.69	$\frac{3}{2}^+$	...	0.44	0.35 (0.52)	0.40 (0.34)	
3.41, 3.06	$\frac{3}{2}^-$	0.60	0.66	0.40 (0.35)	...	
3.97, 3.71	$\frac{1}{2}^-$	...	1.62	1.04 (1.00)	1.00 (1.50)	

[a] T. A. Schmick, K. W. Kemper, P. K. Bindal, and R. D. Koshel, Phys. Rev. C 10, 556 (1974).

[b] B. Cŭjec, Phys. Rev. 136, B1305 (1964).

[c] This work.

[d] S. G. Buccino, D. S. Gemmell, L. L. Lee, J. P. Schiffer, and A. B. Smith, Nucl. Phys. 86, 353 (1966).

from the (^{7}Li, ^{6}Li) reaction for allowed transitions are in good agreement with ^{24}Mg$(d,p)^{25}$Mg studies. Unfortunately, detailed studies of light-ion proton transfer reactions on ^{24}Mg have not been reported so that corresponding comparisons with the (^{7}Li, ^{6}He) reaction were not possible. However, the spectroscopic factors obtained for the analog states of ^{25}Mg and ^{25}Al with the ^{7}Li induced reactions are quite similar. This study of the single nucleon transfer reactions demonstrated that the forward angle (^{7}Li, ^{6}He) data exhibits a j dependence between $d_{5/2}$ and $d_{3/2}$ final states.

The most significant difference between the ^{7}Li induced transfer reactions and light-ion transfer reactions on ^{24}Mg is that the shape of the calculated angular distributions is out of phase with the data. For several states, the phase problem made it difficult to extract spectroscopic factors. It is possible that the phase problem is a result of two-step contributions[25] or the need for a nonlocal optical model potential.[26] Similar transitions will be investigated on spherical nuclei to determine if the phase difficulty is present. The magnitudes of the cross section of the j-forbidden states were much smaller than observed in (d,p) studies, indicating that the contributions from the two-step reaction channels are either destructively interfering or their magnitude is much smaller. Multi-step calculations for the transitions to the j-forbidden states were not pursued at present, because of the long computation times necessary. However, the reduced magnitude of these transitions when compared with the (d,p) reaction makes these calculations of interest, and they will be investigated.[27]

ACKNOWLEDGMENTS

[1] D. Braunschweig, T. Tamura, and T. Udagawa, Phys. Lett. 35B, 273 (1971).

[2] R. S. Mackintosh, Nucl. Phys. A170, 356 (1971).

[3] R. O. Nelson and N. R. Roberson, Phys. Rev. C 6, 2153 (1972).

[4] A. W. Obst and K. W. Kemper, Phys. Rev. C 8, 1682 (1973).

[5] T. A. Schmick, K. W. Kemper, P. K. Bindal, and R. D. Koshel, Phys. Rev. C 10, 556 (1974).

[6] R. L. White and K. W. Kemper, Phys. Rev. C 10, 1372 (1974).

[7] E. Heinicke and H. Baumann, Nucl. Instrum. Methods 74, 229 (1969); 58, 125 (1968).

[8]G. D. Gunn, T. A. Schmick, L. Wright, and J. D. Fox, Nucl. Instrum. Methods **113**, 1 (1973).

[9]G. R. Morgan, G. D. Gunn, M. B. Greenfield, N. R. Fletcher, J. D. Fox, D. L. McShan, and L. Wright, Nucl. Instrum. Methods (to be published).

[10]F. G. Perey, Phys. Rev. **131**, 745 (1963); A. W. Obst, private communication.

[11]P. Schumacher, N. Ueta, H. H. Duhm, K. I. Kubo, and W. J. Klages, Nucl. Phys. **A212**, 573 (1973).

[12]G. R. Satchler, in *Proceedings of the International Conference on Reactions Between Complex Nuclei*, edited by R. L. Robinson *et al.* (North-Holland, Amsterdam, 1974), Vol. 2.

[13]J. S. Blair, Phys. Rev. **115**, 928 (1959).

[14]F. Petrovich, private communication.

[15]T. Tamura, Oak Ridge National Laboratory Report No. 4152 (unpublished).

[16]H. R. E. Tjin, A. Djie, K. Mulder, F. Udo, A. Groenveld, L. A. Ch. Koerts, A. D. Hill, and P. E. Hodgson, Nucl. Phys. **A106**, 85 (1968).

[17]J. Eenmag, R. K. Cole, C. N. Waddel, H. S. Sandhu, and R. R. Dittman, Nucl. Phys. **A218**, 125 (1974).

[18]H. Rebel, G. W. Schweimer, G. Schatz, J. Specht, R. Löhken, G. Hausser, D. Habs, and H. Klewe-Nebenius, Nucl. Phys. **A183**, 145 (1972).

[19]A. A. Rush and N. K. Gangaly, Nucl. Phys. **A117**, 101 (1968).

[20]L. A. Charlton and D. Robson, Florida State University Technical Report No. 5 (unpublished).

[21]S. Cohen and D. Kurath, Nucl. Phys. **A101**, 1 (1967).

[22]R. M. DeVries, M. S. Zisman, J. G. Cramer, K. L. Liu, F. D. Becchetti, B. G. Harvey, H. Homeyer, D. G. Kovar, J. Mahoney, and W. von Oertzen, Phys. Rev. Lett. **32**, 680 (1974).

[23]R. L. White, K. W. Kemper, G. D. Gunn, G. E. Moore, and L. A. Charlton, Phys. Lett. **52B**, 179 (1974).

[24]B. Cŭjec, Phys. Rev. **136**, B1305 (1964).

[25]P. Roussel and F. Pougheon, in *Proceedings of the International Conference on Reactions Between Complex Nuclei*, edited by R. L. Robinson *et al.* (North-Holland, Amsterdam, 1974), Suppl.

[26]R. M. DeVries, Bull. Am. Phys. Soc. **19**, 1014 (1974).

[27]T. Udagawa and A. W. Obst, private communication.